

Confinement of fluxons by surface columnar defects in Bi_{1.8}Pb_{0.33}Sr_{1.87}Ca₂Cu₃O_y tapes

Original

Confinement of fluxons by surface columnar defects in Bi_{1.8}Pb_{0.33}Sr_{1.87}Ca₂Cu₃O_y tapes / Mezzetti, Enrica; Gerbaldo, Roberto; Ghigo, Gianluca; Gozzelino, Laura; L., Gherardi. - In: PHYSICAL REVIEW. B, CONDENSED MATTER. - ISSN 0163-1829. - 59:5(1999), pp. 3890-3895. [10.1103/PhysRevB.59.3890]

Availability:

This version is available at: 11583/1400593 since:

Publisher:

APS

Published

DOI:10.1103/PhysRevB.59.3890

Terms of use:

openAccess

This article is made available under terms and conditions as specified in the corresponding bibliographic description in the repository

Publisher copyright

(Article begins on next page)

Confinement of fluxons by surface columnar defects in $\text{Bi}_{1.8}\text{Pb}_{0.33}\text{Sr}_{1.87}\text{Ca}_2\text{Cu}_3\text{O}_y$ tapes

E. Mezzetti, R. Gerbaldo, G. Ghigo, and L. Gozzelino

Istituto Nazionale di Fisica della Materia-U.d.R Torino-Politecnico, Istituto Nazionale di Fisica Nucleare-Sezione di Torino, Politecnico di Torino, C.so Duca degli Abruzzi 24, 10129 Torino, Italy

L. Gherardi

Pirelli Cavi S.p.A, V.le Sarca 222, 20126 Milano, Italy

(Received 26 February 1998; revised manuscript received 8 September 1998)

We study the effects of *surface* columnar defects created along about 5% of the sample thickness by means of 0.25 GeV Au ions at different doses on $\text{Bi}_{1.8}\text{Pb}_{0.33}\text{Sr}_{1.87}\text{Ca}_2\text{Cu}_3\text{O}_y$ high-quality tapes on the vortex dynamics in the sample bulk. Strong phenomena of vortex localization inside the *bulk* are revealed by shifts of the irreversibility lines (IL's) as well as by their after-irradiation shape. The enhanced IL's exhibit specific characteristics, such as a Bose-glass-like behavior up to quite high fields, with a dose-dependent onset point. Moreover, the irreversible regime expands with decreasing defect density. Such results are consistent with the setting up of confined vortices morphologies. Experimental data concerning the IL with the field orthogonal to the columnar defect direction as well as critical current density enhancements are also reported and discussed. [S0163-1829(99)01205-9]

I. INTRODUCTION

The characteristics and the signatures of different vortex lattice phases in high- T_c superconductors are subjects of extensive experimental and theoretical research.¹⁻⁵ These studies are driven by the need to pin the magnetic flux, whose easy motion generates dissipation, especially at temperatures near the nitrogen fixed point (77.4 K).

Irradiation with swift heavy ions induces correlated disorder provided by columnar defects crossing the whole sample^{6,7} or the greatest part of it.⁸ Such defects can pin magnetic vortices in a very efficient way at rather high temperatures, by inducing a sharp Bose-glass phase transition with vortices localized in the pins.⁶ This transition results in a widely shifted irreversibility line^{6,9} (IL) and particular creep regimes.¹⁰ Control of the vortex dynamics can be further enhanced by optimizing the angular dispersion (splay) of tracks.¹¹ An alternative approach to produce splayed columnar defects is to generate fission tracks by means of high-energy proton irradiation.¹² Also in this case, the splay angles must be controlled in order to expand the irreversible regime.¹³ Nelson recently suggested a method to confine the motion of vortices, near the IL.¹⁴ The center of mass of the vortex is kept in place by applying a small alternating ac magnetic field orthogonal to a background dc field. The alternating field drives vortices through alternatively opposite directions,¹⁵ and produces braided structures which prevent creep formation. The procedure is suitable when the temperature is high enough to allow easy motion of a soft structure of correlated vortices along the whole sample.

Recently, we proposed a strategy to pin vortices in bulk materials.^{16,17} This method consists in irradiating only surface layers of bulk materials with heavy ions of relatively low energy (197 Au¹⁶⁺ at 0.25 GeV). In this way, correlated disorder pins vortices in a limited part of their length, while in the remaining part the vortex is allowed to wander, keeping its center of mass roughly in place. We showed that such

a strategy applied to melt-textured bulk $\text{YBa}_2\text{Cu}_3\text{O}_{7-x}$ produces the expected localization phenomena. In particular, it produces the setup of the well-known Bose-glass phase.¹⁸ The most characteristic feature of the experimental results is that the shift of the IL, as well as the critical current density gain, do not depend on the irradiated volume-fraction (ranging from 5 to 13% of the whole sample) but only on the dynamical state before irradiation. The enhancements are the same at the same $(T/T_{\text{irr}}, B/B_{\text{irr}})$ phase point.¹⁹

In this paper we address the matter by studying a material²⁰ with different intrinsic elastic and anisotropic properties, $\text{Bi}_{1.8}\text{Pb}_{0.33}\text{Sr}_{1.87}\text{Ca}_2\text{Cu}_3\text{O}_y$ (henceforth denoted BSCCO-2223).²¹⁻²³ Columnar defects were created on a surface layer of about 5% of the total thickness. Measurements were performed on six well-characterized BSCCO-2223 samples, irradiated by gold ions to have five defect densities corresponding to equivalent fields (matching fields, B_ϕ) ranging from 1 to 5 T.²⁴ The results show that on this compound surface irradiation produces IL shifts of the same order of magnitude as obtained by tracks crossing the whole sample.^{25,26} However, the after irradiation IL's exhibit characteristics particular of the kind of fluxon arrangement allowed by the surface defects topology.

The main characteristics of the after-irradiation irreversibility lines are (i) the shift starts at an onset phase point, depending on the dose; (ii) for fields just above such point, a Bose-glass-like transition is observed up to another phase point where a kink shows up; (iii) the irreversible regime expands with decreasing defect density.

We show that data-fitting parameters are consistent with a picture of vortices pinned in the irradiated part, but wandering and twisting in the remaining part, even though confined in a space determined by the columnar defect distances. Anisotropy is canceled in a large range of fields around the kink. Current density enhancements are in accordance with the main characteristic trends of the IL's and confirm that such particular "buffer" layer can induce confined vortex

morphologies. Moreover, it is very useful in order to shift to higher fields the “collapse” of the vortex lattice inside the bulk.

II. EXPERIMENTAL DETAILS

The samples, all monofilamentary Ag/BSCCO-2223 tapes, were prepared by the powder-in-tube technique. The thickness of the superconducting core was $100\text{ }\mu\text{m}$.²⁰ Because of the limited penetration depth of Au ions in silver, silver was removed on one side of the tape. The critical temperature, as determined from the onset of the diamagnetic signal, is 108 K and it is almost unaffected by irradiation.

0.25 GeV Au^{16+} ion irradiations were made on six twin samples at the 15 MV Tandem XTU facility of the INFN-Laboratori Nazionali di Legnaro (Padova, Italy) with fluences ranging from 0.5×10^{11} to 2.5×10^{11} ions/cm². These fluences correspond to dose equivalent fields B_ϕ , ranging from 1 to 5 T. The beam direction was parallel to the c axis.

As estimated by means of a TRIM code simulation,²⁷ 0.25 GeV ^{197}Au ions produce columnar defects about $5\text{ }\mu\text{m}$ long in our BSCCO-2223 samples. Above this length, the energy released to target electrons is underthreshold for the formation of columnar defects,^{13,28} but some linear correlation between the defects is expected up to implantation at about $15\text{ }\mu\text{m}$. For high-energy gold ions the estimated defect diameter ranges from 16 to 6 nm, as a function of the penetration depth.^{29,30}

The irreversibility lines of the set of six samples were determined before irradiation and the overlapping of the curves within the experimental errors was verified. Five samples, irradiated at different fluences, were characterized with the magnetic field parallel to the ion tracks in order to determine IL's and enhancements of the critical current density J_c . The sixth sample was irradiated at $B_\phi = 2\text{ T}$ and characterized for both magnetic field orientations (field parallel or perpendicular to the ion tracks) in order to check the anisotropy properties.

All the magnetic characterizations were performed by means of a Lakeshore 7225 magnetometer/susceptometer. The irreversibility lines were determined by the onset of susceptibility third harmonic³¹ at 1000 Hz, while the current densities were evaluated from isothermal dc hysteresis loops.

III. EXPERIMENTAL RESULTS AND DISCUSSION

Figure 1 shows B_{irr} vs T curves for five twin samples irradiated at five different fluences. The magnetic field was applied parallel to the ion tracks. Unlike what happens for tracks crossing the whole sample,¹³ the irreversible regime expands with decreasing defect density in the range of the investigated fluences, from $B_\phi = 5\text{ T}$ to $B_\phi = 1\text{ T}$. The after irradiation IL's exhibit features usually related to fluxon localization.³² However it must be stressed that in our defect topology the irradiated samples show localization phenomena only above an onset phase point $(T_{\text{on}}, B_{\text{on}})$.³³ As the field increase above this point, all the curves show a kink, which is a signature of the Bose-glass transition. We focus our analysis on the region between the onset and such kink.

The crossover fields B_{kink} ,^{6,9,18} between the two regimes corresponding to the higher and weaker localization regions,

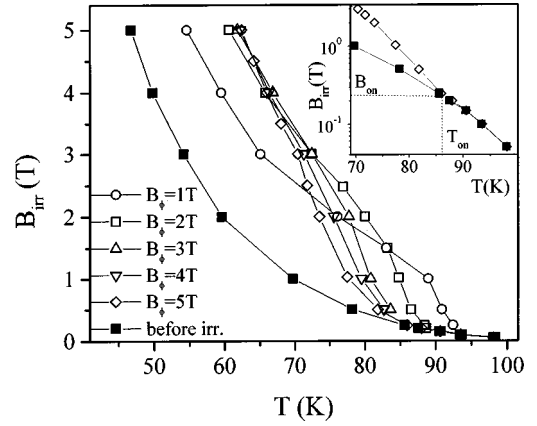


FIG. 1. Irreversibility lines for the unirradiated sample and for samples irradiated with different doses, ranging from $B_\phi = 1$ –5 T. In the inset the onset phase point $(B_{\text{on}}, T_{\text{on}})$ is indicated for the sample with $B_\phi = 5\text{ T}$.

respectively, and the onset field B_{on} , can be better highlighted in the log-log plot of Fig. 2. One can check how all the IL's measured before and after irradiation follow, in the range of fields considered, the law $B_{\text{irr}} \propto (1 - T/T_c)^\alpha$, with different values of the exponent α for different dynamical regimes. In logarithmic scales B_{irr} vs $(1 - T/T_c)$ of Fig. 2, the different regimes result indeed in different linear slopes. The kink is found as the crossing point between the curves with exponents α'' and α''' . In Fig. 2 are indicated both the onset and the kink of the sample irradiated with $B_\phi = 5\text{ T}$. The position of the kink is shifted towards lower reduced temperature, $t = T/T_c$, and reduced field, B/B_ϕ , as the density of tracks increases (Fig. 3).

We conjecture that for $B_{\text{on}} < B < B_{\text{kink}}$ the vortices are localized on tracks in the irradiated part of the sample, while in the remaining part they are allowed to wander, roughly keeping their center of mass in place.

In order to check the above hypothesis and to compare our phase diagram with the diagrams for percolating tracks (thoroughly investigated), we perform the analysis suggested in Ref. 6. Such an analysis is based on the assumption that

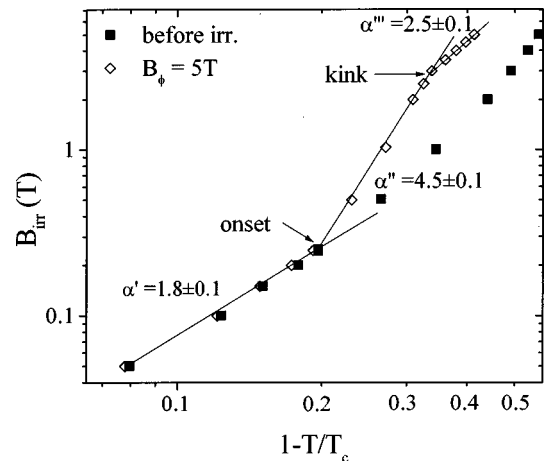


FIG. 2. Irreversibility lines for the unirradiated sample and for samples irradiated with $B_\phi = 5\text{ T}$. The linear slope in the log-log plot gives the exponents in a $B_{\text{irr}} \propto (1 - T/T_c)^\alpha$ law. The onset and the kink (see text) for the irradiated sample are also indicated.

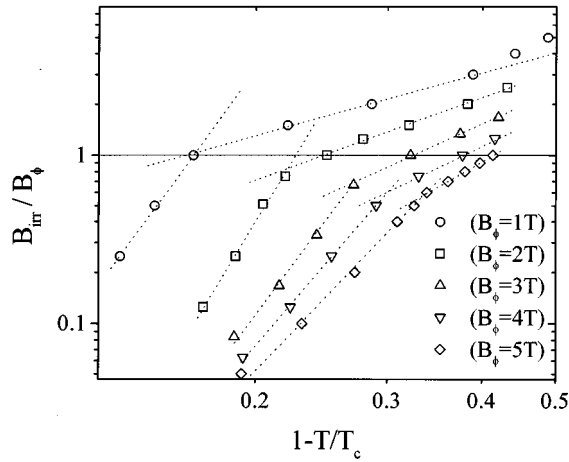


FIG. 3. Irreversibility fields B_{irr} normalized to B_ϕ as a function of $(1 - T/T_c)$, for different irradiation doses. The position of the kink is shifted towards lower reduced temperature $t = T/T_c$, and reduced field B/B_ϕ , as the density of tracks increases.

the vortices are allowed to lay within columnar tubes of a given size.² An analytic expression of the IL for $B < B_{\text{kink}}$ is then derived by

$$t_{\text{BG}} \cong \frac{t_m(B) + \gamma(1 - b)}{(1 + \gamma)}, \quad (1)$$

where $t_{\text{BG}} = T_{\text{BG}}/T_c$ is the Bose-glass reduced temperature and $t_m = T_m/T_c$ is the reduced melting temperature; $b = B/B_{c2}(0)$,

$$\gamma = \frac{b_0^2/(16d)}{\xi_{ab}(0)\sqrt{\text{Gi}}};$$

b_0 is the defect diameter, d is the average distance between tracks, and Gi the Ginzburg number.² In order to take into account the experimental findings of the existence of an onset point, we assumed a Bose-glass-like behavior with dose-dependent onset, modifying Eq. (1) by the introduction of a parameter A . Upon renaming the irreversibility temperature in this confinement regime as T_{conf} , with $t_{\text{conf}} = T_{\text{conf}}/T_c$:

$$t_{\text{conf}}(B) \cong \frac{t_m(B) + \gamma(1 - b)}{(1 + \gamma)} - A.$$

Moreover we observed that the IL of the irradiated sample coincides with the $T_m(B)$ curve for fields lower than B_{on} and temperatures higher than T_{on} , namely the $(T_{\text{on}}, B_{\text{on}})$ point belongs to both $T_m(B)$ and $T_{\text{conf}}(B)$ curves (see inset of Figs. 1 and 2). This condition finally gives $A = \gamma(1 - b - t_{\text{on}})/(1 + \gamma)$ and

$$t_{\text{conf}}(B) \cong \frac{t_m(B) + \gamma t_{\text{on}}}{(1 + \gamma)} \quad (2)$$

with $t_{\text{on}} = T_{\text{on}}/T_c$. We fitted our data by means of Eq. (2), with γ and t_{on} as fitting parameters and assuming the preirradiation irreversibility line as a good estimate of $t_m(B)$. Figure 4 shows the resulting fit for the $B_\phi = 5$ T sample, while in Table I are reported the fitting parameters for all samples including the sample irradiated at lower fluence.

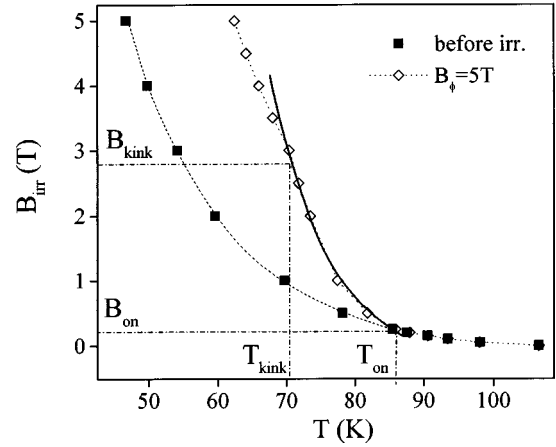


FIG. 4. Irreversibility lines for the unirradiated sample and for samples irradiated with $B_\phi = 5$ T. The solid line is a fit of the experimental data, between B_{on} and B_{kink} , with Eq. (2) (see text).

This value has been included notwithstanding the quite low number of available experimental points because the general trend is nicely followed. The parameter γ in our case is crucial, in that it relates the interdefect distance d and the confinement diameter b_0 , which we do not assume *a priori* to be the equal of the defect diameter. In order to obtain b_0 from γ we selected $\xi_{ab}(0) = 14$ Å (Ref. 34) and $\text{Gi} = 0.1$.² A single value of b_0 for the different doses could not be found. Table I shows the values of b_0 at different values of B_ϕ . The order of magnitude of the fluence-dependent b_0 is in average higher than the diameter of gold-ion columnar defect reported by Zhu *et al.*²⁹ and this conclusion does not depend on the particular value chosen for $\xi_{ab}(0)$. In Table I the average distances between defects at the respective irradiation doses are reported for comparison. Considering that b_0 roughly scales with the irradiation dose as the interdefect distance, we interpret the fitted values of b_0 as a diameter of the vortex “confinement” cross section, which now takes the place of the columnar defect cross section. b_0 represents the transverse size of the vortex bundle with a part pinned into columnar defects near the IL. Different sizes are allowed for different doses and the smaller ones correspond to higher fluences.

In order to perform a more detailed investigation of the main characteristics of the vortex phase induced by the surface defect topology, we analyze the results by means of a further comparison with the analysis mentioned above.

In Ref. 35 the IBM group expressed the pinning efficiency η for Y-Ba-Cu-O as $\eta = 0.25/(1 + \varepsilon B_\phi) \propto B^*/B_\phi$, where ε

TABLE I. Values of the fitting parameters γ and t_{on} , relative to Eq. (2) for different irradiation doses B_ϕ . The values of b_0 , deduced from γ with $\xi_{ab}(0) = 14$ Å (see text), and d , the average distance between defects, are also reported.

B_ϕ (T)	γ	t_{on}	b_0 (nm)	d (nm)
1	3.61 ± 0.12	0.885 ± 0.001	33.8 ± 0.6	44.7
2	3.26 ± 0.18	0.837 ± 0.002	27.0 ± 0.8	31.6
3	1.77 ± 0.17	0.820 ± 0.006	18.0 ± 0.9	25.9
4	1.50 ± 0.04	0.807 ± 0.002	15.4 ± 0.2	22.4
5	1.06 ± 0.04	0.805 ± 0.004	12.3 ± 0.2	20.0

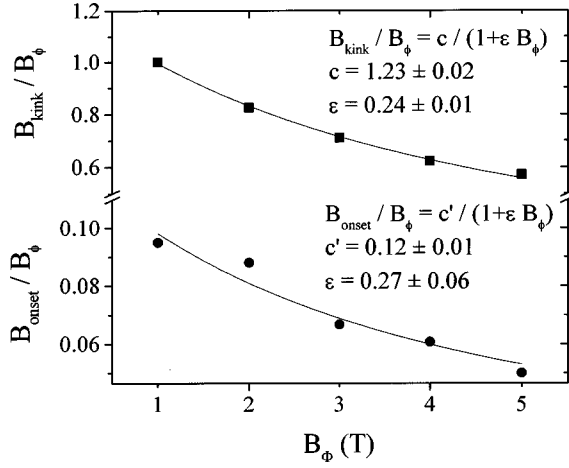


FIG. 5. Field of the kink and field of the onset, normalized to B_ϕ , as a function of B_ϕ . The curves are fits of the data with Eqs. (3) and (4), with the fitting parameters reported in the figure.

$= \pi r^2 / (2\Phi_0)$, πr^2 being the track cluster area, ϕ_0 is the flux quantum, and B^* is the accommodation field, introduced by Nelson.² Our hypothesis is that the field of the kink B_{kink} , is also proportional to B^* in a 3D regime and, as a consequence, that

$$B_{\text{kink}}/B_\phi = \frac{c}{1 + \epsilon \cdot B_\phi}, \quad (3)$$

where c is a constant. We fitted our data by means of this expression, with ϵ and c as fitting parameters. Results are reported in Fig. 5, where the values of the parameters are also indicated. From this analysis results a confinement diameter $2r \approx 36$ nm, of the same magnitude order of the parameter b_0 evaluated above. As previously outlined, in our case $2r$ does not represent the average diameter of track clusters, but rather represents the average transversal dimension of a confined vortex line. In this kind of fit the value of r obviously is the result of a spatial averaging as well as of an averaging over different B_ϕ . The order of magnitude of the value obtained confirms this interpretation in relation with the analysis by Eq. (2). Also the lower limit of the confinement region B_{on} fits the same dose dependence. In Fig. 5 is reported a fit of the data with the expression

$$B_{\text{on}}/B_\phi = \frac{c'}{1 + \epsilon \cdot B_\phi}, \quad (4)$$

similar to Eq. (3). The value of the parameter ϵ , i.e., the value of the confinement radius, is, within errors, the same as in the previous case. We can therefore conclude that, in our case, $B_{\text{on}} \propto B_{\text{kink}} \propto \eta B_\phi$.

Figure 6 reports the curve B_{kink}/B_ϕ as a function of $(1 - T/T_{\text{on}})$. The fit of data with $B_{\text{kink}}/B_\phi \propto (1 - T/T_{\text{on}})^\beta$ gives the value $\beta \approx 1/2$, suggesting the existence of a longitudinal correlation length vanishing at $T = T_{\text{on}}$, and not at $T = T_c$. This phenomenological parameter is expected to be proportional to the longitudinal size of coherently pinned segments of vortices at a given dose.³³

Au-ion irradiation caused a marked reduction of IL anisotropy as well as of J_c anisotropy, as shown in Fig. 7. In particular, the IL's shift measured for B parallel to the ion

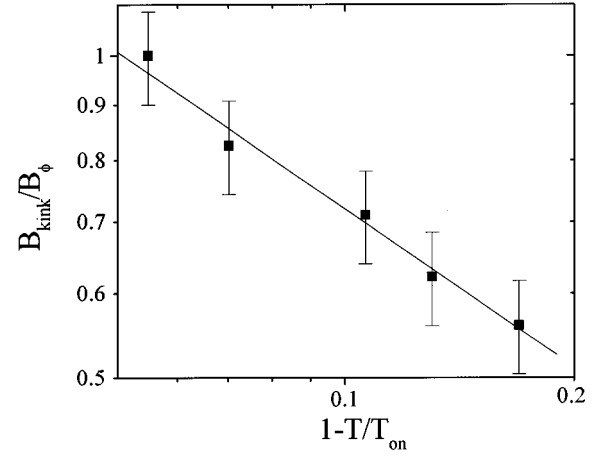


FIG. 6. B_{kink}/B_ϕ as a function of $(1 - T/T_{\text{on}})$, on logarithmic scales. The fit of data with the law $B_{\text{kink}}/B_\phi \propto (1 - T/T_{\text{on}})^\beta$ gives the value $\beta = 0.49 \pm 0.03$.

tracks turned out to be the right one to produce full overlap with the IL measured for B perpendicular from a point phase just above $(T_{\text{on}}, B_{\text{on}})$ up to fields higher than B_{kink} . The IL measured for B perpendicular to the ion tracks remained almost unchanged. The overall effect is the abatement of the IL anisotropy after irradiation, at high temperature and rather high field.

It has been already suggested in the literature that irreversibility lines measured by means of ac methods are in accordance with the IL's produced by transport measurements,³⁶ because in both kinds of measurements the same relaxation time window is involved. On the contrary, especially for BSCCO-2223, dc magnetic measurements do not only underestimate J_c strongly with respect to what can be expected from transport measurements,³⁶ but also the error rate depends on the *a priori* different creep regime involved. Because of this, for BSCCO-2223 tapes it is somehow wrong to compare J_c before and after irradiation evaluated by means of the amplitude of the dc magnetization loop at a given field. However, these measurements offer some further information concerning how surface defects operate. In fact, the “apparent” enhancements of the measured

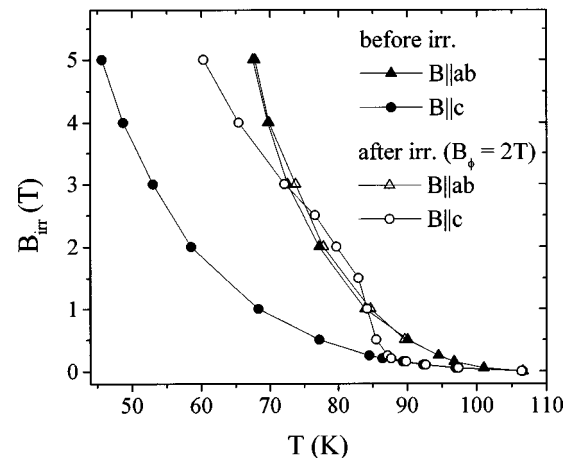


FIG. 7. Comparison of the anisotropy of IL's before and after irradiation, for the magnetic field applied parallel and perpendicular to ion tracks, i.e., to the c axis of the samples.

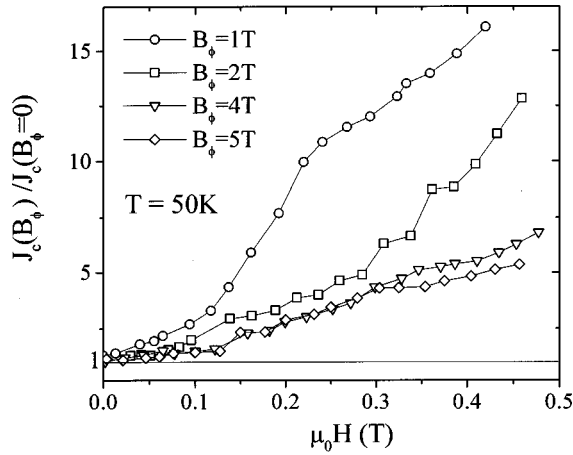


FIG. 8. Critical current enhancements as a function of the applied field, for different irradiation doses.

currents at a given B_ϕ increase with temperature and are in a qualitative accordance with the IL behavior as a function of fluence (Fig. 8).

In addition and in accordance with previous results,¹⁹ at rather high temperature these kinds of defects produce the recovering of an ultrafast decay of the currents to a decay approximately following a $1/H$ law (Fig. 9). Due to the fact that the currents before and after irradiation are estimated at a given field after the same time delay, we can deduce that such defects strongly reduce the creep rate. In other words, an apparent regime very near to collapse of the vortex matter is transformed into a collective-pinning regime with $1/H$ behavior³⁷ which is the signature of a regime dominated by elastic energy. In our case the columnar pinning energy acting just along a small part of the full length of the sample is not sufficient to avoid wandering in the affected part, but provides a restoring force. This force is high enough to avoid segments of longitudinally correlated vortices to diffuse through the sample.³³

IV. CONCLUSIONS

The main achievement of this work is showing that surface columnar defects affect the dynamics of the underlying

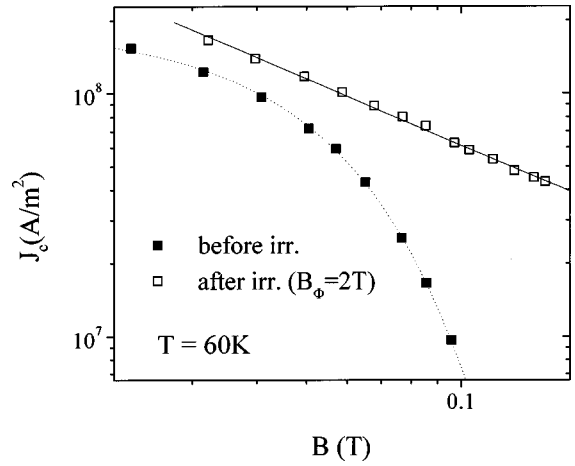


FIG. 9. Critical current density before and after $B_\phi = 2$ T irradiation. The solid line is a fit of the data with the law $J_c \propto H^\delta$. We found $\delta = -0.91 \pm 0.03$.

bulk layer by inducing local confinement of the fluxon lattice, starting at a dose-dependent phase point. In particular, lateral wandering is allowed inside tubes whose cross section b_0 is dose dependent. Another underlying relevant phenomenological parameter could be a longitudinal correlation length, which vanishes at $T = T_{on}$. At least the first parameter acts as a boundary condition for the allowed morphologies of the fluxon arrangements at a given dose.

In summary, the particular strategy involved in surface irradiation “*de facto*” employs in the bulk the very low elastic energy surviving at high temperatures, with just a little external energy supply due to surface columnar defects, to obtain somewhat ordered vortex morphologies.³⁸ The matter is worthy to be extensively investigated, both from a fundamental and technological point of view.

ACKNOWLEDGMENTS

The authors wish to thank P. Caracino, M. Rasetti, and A. Tagliacozzo for meaningful discussions. The authors also acknowledge the technical support of the L.N.L. staff as well as the financial support of A.S.P. (Associazione per lo Sviluppo Scientifico e Tecnologico del Piemonte).

¹D. R. Nelson and V. M. Vinokur, Phys. Rev. Lett. **68**, 2398 (1992).

²D. R. Nelson and V. M. Vinokur, Phys. Rev. B **48**, 13 060 (1993).

³T. Hwa, P. Le Doussal, D. R. Nelson, and V. M. Vinokur, Phys. Rev. Lett. **71**, 3545 (1993).

⁴L. Balents and M. Kardar, Phys. Rev. B **49**, 13 030 (1994).

⁵U. C. Tauber and D. R. Nelson, Phys. Rev. B **52**, 16 106 (1995).

⁶L. Krusin-Elbaum, L. Civale, G. Blatter, A. D. Marwick, F. Holtzberg, and C. Feild, Phys. Rev. Lett. **72**, 1914 (1994).

⁷L. Civale, A. D. Marwick, T. K. Worthington, M. A. Kirk, J. R. Thompson, L. Krusin-Elbaum, Y. Sun, J. R. Clem, and F. Holtzberg, Phys. Rev. Lett. **67**, 648 (1991); W. Gerhäuser, G. Ries, H. W. Neumüller, W. Schmidt, O. Eibl, G. Saemann-Ischenko, and S. Klaumünzen, *ibid.* **68**, 879 (1992); V. Hardy, Ch. Simon, J. Provost, and D. Groult, Physica C **205**, 371

(1993); L. Civale, L. Krusin-Elbaum, J. R. Thompson, R. Wheeler, A. D. Marwick, M. A. Kirk, Y. R. Sun, F. Holtzberg, and C. Feild, Phys. Rev. B **50**, 4102 (1994).

⁸L. Civale, A. D. Marwick, R. Wheeler, M. A. Kirk, W. L. Carter, G. N. Riley, and A. P. Malozemoff, Physica C **208**, 137 (1993).

⁹V. Hardy, Ch. Simon, J. Provost, and D. Groult, Physica C **205**, 371 (1993).

¹⁰J. R. Thompson, L. Krusin-Elbaum, L. Civale, G. Blatter, and C. Feild, Phys. Rev. Lett. **78**, 3181 (1997).

¹¹L. Krusin-Elbaum, A. D. Marwick, R. Wheeler, C. Feild, and V. M. Vinokur, Phys. Rev. Lett. **76**, 2563 (1996).

¹²L. Krusin-Elbaum, D. Lopez, J. R. Thompson, R. Wheeler, J. Ullmann, C. C. Tsuei, C. W. Chu, and Q. M. Lin, Physica C **282-287**, 375 (1997); L. Krusin-Elbaum, D. Lopez, J. R. Thompson, R. Wheeler, J. Ullmann, C. W. Chu, and Q. M. Lin,

- Nature (London) **389**, 243 (1997).
- ¹³L. Civale, Supercond. Sci. Technol. **10**, A11 (1997).
 - ¹⁴D. R. Nelson, Nature (London) **385**, 675 (1997).
 - ¹⁵M. V. Indenbom, C. J. van der Beek, V. Berseth, W. Benoit, G. D'Anna, A. Erb, E. Walker, and R. Flukiger, Nature (London) **385**, 702 (1997).
 - ¹⁶E. Mezzetti, R. Cherubini, R. Gerbaldo, G. Ghigo, L. Gozzelino, and B. Minetti, Nuovo Cimento D **18**, 1099 (1996).
 - ¹⁷E. Mezzetti, R. Gerbaldo, G. Ghigo, L. Gozzelino, B. Minetti, and R. Cherubini, IEEE Trans. Appl. Supercond. **7**, 1993 (1997).
 - ¹⁸E. Mezzetti, R. Gerbaldo, G. Ghigo, L. Gozzelino, B. Minetti, and R. Cherubini, Physica C **282-287**, 2095 (1997).
 - ¹⁹E. Mezzetti, R. Gerbaldo, G. Ghigo, L. Gozzelino, B. Minetti, and R. Cherubini, J. Appl. Phys. **82**, 6122 (1997).
 - ²⁰L. Gherardi, P. Caracino, G. Coletta, and S. Spreafico, Mater. Sci. Eng., B **39**, 66 (1996).
 - ²¹P. Kummeth, C. Struller, H. W. Neumuller, G. Saemann-Ischenko, and O. Eibl, *Critical Currents in Superconductors*, edited by H. W. Weber (World Scientific, Singapore, 1994), p. 311.
 - ²²T. Matsushita, Physica C **214**, 100 (1993).
 - ²³M. Kiuchi, H. Yamato, and T. Matsushita, Physica C **269**, 242 (1996).
 - ²⁴The dose equivalent field is the magnetic field which would be ideally required to fill each track with a flux quantum, i.e., $B_\Phi = n\Phi_0$, where Φ_0 is the flux quantum and n is the track density.
 - ²⁵R. Gerbaldo, G. Ghigo, L. Gozzelino, E. Mezzetti, B. Minetti, P. Caracino, and L. Gherardi, in *Applied Superconductivity 1997*, edited by H. Rogalla and D. H. A. Blank, Inst. Phys. Conf. Ser. No 158 (IOP, London, 1997), p. 1101.
 - ²⁶D. Zech, S. L. Lee, H. Keller, G. Blatter, B. Janossy, P. H. Kes, T. W. Li, and A. A. Menovsky, Phys. Rev. B **52**, 6913 (1995).
 - ²⁷J. F. Ziegler, J. P. Biersack, and U. Littmark *The Stopping and Range of Ions in Solids* (Pergamon, New York, 1985), Vol. 1.
 - ²⁸V. Hardy, J. Provost, D. Groult, Ch. Simon, M. Hervieu, and B. Raveau, J. Alloys Compd. **195**, 395 (1993).
 - ²⁹Y. Zhu, R. C. Budhani, Z. X. Cai, D. O. Welch, M. Suenaga, R. Yoshizaki, and H. Ikeda, Philos. Mag. Lett. **67**, 125 (1993).
 - ³⁰D. X. Huang, Y. Sasaki, S. Okayasu, T. Aruga, K. Hojou, and Y. Ikuhara, Phys. Rev. B **57**, 13 907 (1998).
 - ³¹E. R. Yacoby, A. Shaulov, Y. Yeshurun, M. Konczykowski, and F. Rullier-Albenque, Physica C **199**, 15 (1992).
 - ³²D. Zech, S. L. Lee, H. Keller, G. Blatter, P. H. Kess, and T. W. Li, Phys. Rev. B **54**, 6129 (1996).
 - ³³D. Giller, A. Shaulov, R. Prozorov, Y. Abulafia, Y. Wolfus, L. Burlachkov, Y. Teshurun, E. Zeldov, V. M. Vinokur, L. J. Peng, and R. L. Greene, Phys. Rev. Lett. **79**, 2542 (1997).
 - ³⁴W. C. Lee and D. M. Ginsberg, Phys. Rev. B **44**, 2815 (1991); W. C. Lee, J. H. Cho, and D. C. Johnston, *ibid.* **43**, 457 (1991).
 - ³⁵L. Krusin-Elbaum, L. Civale, J. R. Thompson, and C. Feild, Phys. Rev. B **53**, 11 744 (1996).
 - ³⁶L. Martini, A. Gandini, L. Rossi, V. Ottoboni, and S. Zannella, Physica C **261**, 196 (1996).
 - ³⁷G. Blatter, M. V. Feigel'man, V. B. Geshkenbein, A. I. Larkin, and V. M. Vinokur, Rev. Mod. Phys. **66**, 1125 (1994).
 - ³⁸F. J. Nédélec, T. Surrey, A. C. Maggs, and S. Leiber, Nature (London) **385**, 305 (1997).